CHAPTER VII

INFLUENCES OF CATALYST TEMPERATURES AND Ru-LOADED CATALYSTS ON WASTE TIRE PYROLYSIS AND ITS PRODUCTS

7.1. Abstract

This paper investigates the effects of Ru/MCM-41 catalysts in the pyrolysis of waste tire using a semi-batch reactor. The pure silica support MCM-41 was synthesized *via* silatrane route. Prior to evaluating the activity of Ru/MCM-41 catalysts, the influences of MCM-41 in relation with catalyst temperature were studied. The results indicated a strong impact of catalyst temperatures on the yield and nature of pyrolysis products. Oil yield first decreased then increased with catalyst temperature. However, the highest catalyst temperature produced the oil that has higher poly-aromatic content. Ru/MCM-41 catalyst produced much lighter oil and dramatically decreased the concentration of poly- and polar-aromatics in the oil but also decreased the yield of oil. And the catalytic activity of Ru/MCM-41 was found to increase with Ru content in the tested range of ruthenium loading. The increase in catalytic activity was discussed in relation with catalyst characterizations.

7.2. Introduction

Tires are designed to be resistant to chemical, biological and physical degradation. Owing to their low bulk density, they occupy large volumes and, if buried, disrupt the integrity of landfill sites. Meanwhile, the world production of waste tire is approximate $6x10^6$ tons/year, and nearly 70% of these waste are simply dumped in the open or in the land-filled [1,2]. Moreover, fires at tire deposits have been reported to be very difficult to control and generate high levels of pollution to the soil, atmosphere and waters [3].

In many countries, the environmental regulations concerning the waste tire are becoming more and more stringent. This waste hierarchy favors the valorization and recycling alternatives. Thus, over recent years, tire pyrolysis, a recycling process, has attracted renewed significant attention. It essentially involves degradation of the

tire components by exposure to high temperatures in the absence of oxygen. The result is a carbonized char, condensable oil and a gas fraction. Gas fraction has been reported to have high calorific value [4], and high hydrogen content [2,5,6], whereas the tire-derived oil was shown to be similar, to a certain extent, to the commercial petroleum naphtha [7]. However, the high concentration of aromatic hydrocarbons (HCs) [7-9], especially polycyclic HCs (PAHs), has limited its application as a fuel. As a result, several studies have been done with focusing on the possibilities for the production of chemical feedstock from the tire-derive oil rather than fuel. For instance, Williams and Brindle [10,11] and Boxiong *et al.* [12] reported the high selectivity toward single ring aromatic HCs in the light fractions by catalytic pyrolysis of waste tire using ZSM-5 and USY zeolites as catalysts, respectively. Our previous study [13], a first step in the attempts to study the possibility of fuel production from waste tire, has shown that the mordenite-catalyzed pyrolysis of waste tire produced the oil having high selectivity toward gasoline, kerosene and gas oil fractions. However, a relative high amount of poly- and polar-aromatics still existed in the oil. And, the amount of aromatics increased with increasing acid properties of the catalyst. As a result, a new catalyst should be rationally designed and tested for waste tire-to-fuel process.

Bifunctional catalysts are extensively studied for aromatic reduction [14]. Metals can catalyze the hydrogenation of the feedstock, making it more reactive for cracking and heteroatoms (sulfur, oxygen) removal [15]. And a high level of aromatic hydrogenation at moderate hydrogen pressures can be achieved with noble metals catalysts [16,17]. The intrinsically high hydrogenation activity of noble metal might help reducing steric effects that impede the direct elimination of the sulfur heteroatom [18,19]. However, noble metals display a low resistance to sulfur poisoning limiting their applications. The sulfur tolerance of a noble metal supported catalyst may be enhanced by (i) using acidic carriers [20], (ii) changing the metal particle size, or (iii) alloying with other metals [21]. Considering the metallic nature, Ru was reported to have a better sulfur tolerance than Pt, Pd or Pd-Pt catalysts due to the low density of states at the Fermi level of this metal [22]. On the other hand, due to the size of the aromatic molecules, especially the PAHs, a large pore material consequently should be used as the support of the bifunctional catalyst. Pure silica

MCM-41, which has a mild acidic property, was shown to exhibit good activity for the degradation of waste plastic [23-25]. The carbon number distribution of the derived oil shifted to lower number, and the authors also observed the carbenium ion cracking mechanism over this material [25]. Besides, catalytic temperature strongly affected the products obtained from catalytic pyrolysis of waste tire [10,26].

The aim of this work is to investigate the influences of Ru-supported pure silica MCM-41 catalyst on the products obtained from waste tire pyrolysis. For this purpose, a pure silica MCM-41 was synthesized *via* silatrane route. Then, pyrolysis of waste tire using MCM-41 as a catalyst was conducted to study the effects of catalytic temperature to find the optimum condition. Subsequently, a series of Ru-supported catalysts, prepared by impregnation technique with various Ru loading, were subjected to waste tire pyrolysis to evaluate their influence on the yields and the nature of the evolved products.

7.3. Experimental

7.3.1 Catalyst Preparation

To synthesize pure silica MCM-41, silatrane was first synthesized using the method of Wongkasemjit's group [27]. The silatrane precursor was added to a solution containing CTAB, NaOH, and TEA, followed by adding water with vigorous stirring [28]. The obtained crude product was filtered and washed with water to obtain a white solid. Then, the white solid was dried at room temperature and calcined at 580oC for 6 hours to obtain mesoporous MCM-41.

Ru-supported catalysts were prepared by the conventional wetness impregnation technique. An appropriate amount of precursor solution of $RuCl_3.xH_2O$ (FLUKA) was loaded to the MCM-41, followed by drying in an oven at 110°C for 3 hours, and then calcined at 580°C for 2 hours. Subsequently, it was pellitized and sieved to obtain particle sizes in the range of 400- 425 μm. Prior to catalytic activity testing, each catalyst was reduced by hydrogen at 400°C for 3 hours.

7.3.2 Catalyst Characterization

XRD patterns were obtained using the Riguku D/Max 2200H with a scanning speed of 0.5 degree/min and 2θ from 1.5 degree to 60 degree. The

composition of the Ru on the support was determined by the Inductively Coupled Plasma (ICP) technique using a Perkin Elmer Optima 4300 PV machine. The surface area and pore size distribution of the studied catalysts were characterized by N_2 physical adsorption using a Sorptomatic 2900 equipment. Hydrogen chemisorption at room temperature was carried out in a Micromeritics 2900 apparatus, after the *in-situ* reduction of sample at 500°C (10°C.min^{-1}) for 1 hour, under a flow of H_2. Dispersion data was calculated by assuming a stoichiometry H/Ru =1 [17]. Temperature-programmed desorption (TPD) using NH_3 was carried out in a TPD/TPR Micromeritics 2900 machine. Approximately 0.1g of sample was first pretreated in He at 550°C for 30 minutes. Then, the system was cooled to 100°C, and the NH_3 adsorption was performed using NH_3/N_2 for 1.5 hours followed by the introduction of He to remove the physically adsorbed NH_3 for 30 minutes at 100°C. Finally, the system was cooled to 50°C, and then the temperature program desorption was started from 50°C to 600°C with a heating rate of 5°C/min. TPR of Ru-supported catalysts was conducted using the same Micromeritic 2900 equipment from room temperature to 500°C with a heating rate of 5°C/min. Temperature program oxidation (TPO) using also the Micromeritics 2900 machine was performed from room temperature to 900°C (10°C/min), and the final temperature was held for 30 minutes. The amount of coke was then determined from the area under the curve and calculated by the software supplied with the machine.

7.3.3 Pyrolysis of Waste Tire

The detail of pyrolysis process was described elsewhere [13]. Briefly, the pyrolysis of waste tire was carried out in the lower zone of the reactor, where the temperature was set at 500°C. Then, the evolved product was carried by a nitrogen flow to the upper zone packed with a catalyst. This zone was controlled at various catalytic temperatures (350, 400 and 450°C) in order to investigate the influence of catalytic temperature. The obtained product was next passed through an ice-salt condensing system containing 3 condensers in order to separate incondensable compounds from the liquid product. The solid and liquid products were weighed to determine the product distribution. The amount of gas was then determined by mass balance. Prior to being analyzed, the liquid product was dissolved in n-pentane to precipitate asphaltenes. The obtained maltenes was analyzed by FTIR and liquid

adsorption chromatography [29]. In the later process, saturated hydrocarbons, mono-, di-, poly- and polar aromatics in the maltenes were fractionated. Finally, a Varian CP 3800 Simulated Distillation Gas Chromatograph (SIMDIST GC) equipped with FID was used to analyze the obtained maltene and hydrocarbon fractions according to the ASTM D2887 method to determine simulated true boiling point curves. The petroleum fractions were then cut based on their boiling point, including naphtha (<200°C), kerosene (200°C-250°C), gas oil (250°C – 370°C) and residue (>370°C).

7.4 Results and Discussion

7.4.1 Catalyst Characterization

Figure 7.1 illustrates the XRD patterns of the synthesized MCM-41 and Ru-supported samples. As seen in the figure, the structure of MCM-41 does not change after incorporation of ruthenium and no peak of ruthenium species is observed. Probably the amount of Ru loaded is below the detectable range of the XRD equipment and/or ruthenium is highly dispersed in all samples.

The physical properties of the fresh catalysts and the amount of coke of the used ones are summarized in Table 7.1. Accordingly, ICP analysis indicates a very good consistence between the targeted and true values of metal loaded in all samples. The BET surface area of silica MCM-41 is very high, and the average pore diameter is approximately 2.6 nm, which is similar to the values reported in [28]. H_2-chemisorption results show that the mean diameter of ruthenium particles for all samples is about 1.9 nm, and the diameter increases with increasing ruthenium loading. In addition, all Ru-supported samples have a high metal dispersion of 65.2-68.5%. However, the dispersion of ruthenium slightly decreases with increasing concentration of ruthenium in the sample. Furthermore, the incorporation of Ru slightly decreases the surface area of the support in association with a reduction in average pore diameter, possibly caused by the diffusion of Ru into the pore.

The strength and distribution of acid sites of all prepared catalysts determined by TPD-NH_3 are given in Figure 7.2. It can be seen that the profile of MCM-41 shows 2 desorption peaks with maxima at 150°C and 350°C, respectively. These peaks are broad and low intensive suggesting a good distribution of the acidic

sites as well as the low amount of acidic sites. As this zeolite material is composed of pure silica; thus, the acid sites must be contributed from the silanol groups lining the wall of the channels as suggested by Seddegi et al. [25]. The incorporation of ruthenium slightly decreases the intensity of the peaks, possibly caused by the diffusion of ruthenium particles into the zeolite channels, thus blocking some acidic sites. The total acid sites of Ru-supported catalysts are comparable.

Figure 7.3 depicts the TPR profiles of all samples. Accordingly, the locations of the peaks in TPR profiles of all samples with different Ru loadings are similar, but the intensity increases with increasing Ru content. And, Ru-supported MCM-41 exhibits a main reduction peak at 190°C, which is higher than Ru-supported on mesoporous silica doped with zirconium [30], indicating a stronger metal support interaction. Consequently, from H_2-chemisorption analysis the high dispersion of Ru in all Ru-supported samples (>65%) was observed (Table 7.1), which is well consistent with XRD results. Moreover, as indicated in Table 7.1, the amount of coke of the spent catalysts obtained from TPO analysis shows that Ru-supported catalysts produced a higher amount of coke than MCM-41.

7.4.2 Influences of MCM-41 and Catalyst Temperatures

7.4.2.1 Influences of MCM-41

The pyrolysis products obtained from thermal and catalytic pyrolysis over MCM-41 are summarized in Table 7.2. It can be seen that the gas yield obtained from the MCM-41 is much higher than that produced from thermal pyrolysis. In addition, with respect to thermal pyrolysis, the oil generated over MCM-41 has higher naphtha and kerosene, and the poly- and polar-aromatic contents in the oil are lower. These results might be ascribed to the cracking activity of the catalyst [13]. Besides, saturates in the derived oil decreases with using MCM-41. This is well consistent with the results obtained from FTIR analysis, as depicted in Figure 7.4. It can be seen that the infrared absorption bands of interest are observed around the range of C-H stretching vibration of $-CH_2-$ and $-CH_3$ groups approximately between 3,000 and 2,800 cm-1 [31]. The peak at 3,030 cm-1 represents the aromatic C-H stretching, whereas the one at 2920 cm-1 represents the symmetric aliphatic C-H stretching, and the ratio of the two peaks correlates with the aromaticity of the hydrocarbon compounds [32]. And obviously, as compared to

thermal pyrolysis, MCM-41 generated the oil having the higher ratio of $I_{3030cm^{-1}}/I_{2920cm^{-1}}$; thus, it has lower saturated hydrocarbons [31,32].

On the other hand, the use of MCM-41 leads to a dramatic increase in the concentrations of mono- and di-aromatics (Table 7.2). Figure 7.5 illustrates the carbon number distribution of mono- and di-aromatics. Accordingly, MCM-41 causes the shifts of these compounds distribution to higher carbon number, indicating the formation of heavier aromatics. It is well accepted that aromatic hydrocarbons are not easy to be converted in a secondary cracking reaction [33,34]. Meanwhile, alkylation reaction can be promoted by a Lewis acid catalyst [35,36], and MCM-41 was reported to favor the alkylation reaction of previously formed aromatic rings [37]. Therefore, it is proposed that probably MCM-41 promotes not only the cracking of saturated HCs and but also the alkylation of the already-generated aromatics. As a result, heavier mono- and di-aromatics are produced, leading to the increment of mono- and di-aromatic concentration in the tire-derived oils.

7.4.2.2 Influences of Catalyst Temperatures

Table 7.3 summarizes the product yields, the petroleum fractions and compositions of the oils produced by pyrolysis with MCM-41 catalyst at various catalyst temperatures. Accordingly, catalyst temperature does not influence the solid yield since the pyrolysis conditions were kept constant, and the tire was completely decomposed at 500°C [2]. However, catalyst temperature strongly affects the yields of other products. As seen from Table 7.3, the yield of gaseous products first increases at the expense the liquid yield as the catalyst temperature raises from 350°C to 400°C, which is attributed to greater and deeper cracking reactions. Further increasing this temperature to 450°C causes a reduction in the yield of gaseous product in accordance with an increase in the yield of the oil. Liquid adsorption chromatography analysis also shows an increase in poly- and polar-aromatics with catalyst temperature (Table 7.3). Possibly, a considerable amount of olefins including conjugated olefins, aromatics, etc, produced during pyrolysis, might undergo cyclization, alkylation followed by dehydrogenation to produce (heavier) aromatics when the acid catalyst was used [11,38]. Note that these reactions are favored at high reaction temperatures [6] and aromatic content in the

pyrolytic oil increased when a zeolite with a large pore diameter was used [13]. Therefore, the very high catalyst temperature together with the meso-pores of the MCM-41 should be responsible for the increment of liquid yield as well as the formation of heavier aromatics from olefins and/or the lighter ones. On the other hand, it was elucidated that aromatic and alkene species have a greater predisposition to being involved in pathways to coke formation because of their ability to easily be involved in hydrogen transfer and cyclization reactions [39]. As a result, a higher amount of coke is produced as the catalyst temperature rises (Table 7.1). And the high amount of coke formed can cause the deactivation of the catalyst; thus, reducing its cracking activity leading to a reduction in the yield of gas product.

It can be seen in Table 7.3 that, regardless to the catalyst temperature, the yield of naphtha fraction from catalytic pyrolysis is higher than that from thermal pyrolysis. And, the variation in catalyst temperature alters the contents of petroleum fractions in the pyrolytic oils; that is, increasing this temperature decreases naphtha in consistence with an increment in kerosene and gas oil as well as residue, suggesting the existence of the recombination of light molecules and leading to the formation of heavier compounds, and a consequent higher liquid yield. This well coincides with the fact that heavy molecules such as poly- and polar-aromatics jump up at the catalyst temperature of 450°C (Table 7.3). Running at the highest catalyst temperature in the testing range yields the highest amount of gas oil and kerosene. Besides, under the catalyst temperature of 400°C, the production of naphtha, kerosene and gas oil decreases, which is attributed to the high cracking activity under this condition, as mentioned previously.

Since light oils are commercially valuable, from these results together with the fact that aromatic hydrogenation is thermodynamically favored at low temperatures [30], the catalyst temperature of 350°C was selected for further study on the effects of Ru loading.

7.4.3 Effects of Ru-loading Amount

In this section, the effects of Ru supported on pure silica MCM-41 and the amount of Ru loading (1.0, 1.5 and 2% wt) on the yields and nature of the products obtained from pyrolysis of waste tire were studied.

7.4.3.1 Product Distribution

Figure 7.6 illustrates the effects of Ru loading amount on the product distribution. The data of MCM-41 and non-catalytic pyrolysis were also included for comparison purpose. It can be seen that the gas yield increases dramatically at the expense of liquid yield when the catalysts were used, especially the ones with Ru loading. For instance, the gas yield obtained from pyrolysis in the absence of a catalyst is approximately 3 times less than that obtained when 2%Ru/MCM-41 was used. The promotion effects of Ru incorporation on cracking activity might be attributed to the combination of metal and acid properties of the bifunctional Ru-supported MCM-41 catalyst. The high hydrogenation activity of Ru [15] probably hydrogenated aromatic HCs, which were reported to be predominant in the products obtained from pyrolysis of waste tire [7-9,11], and then these hydrogenated compounds might undergo catalytic cracking by MCM-41 producing lighter HCs. Free hydrogen is liberated from the pyrolysis products as reported in many studies [2,5,6], and/or is generated during the reforming reactions [2,6]. As indicated by XRD, and H_2-chemisorption analysis, Ru is highly dispersed in all Ru-supported catalysts. The high dispersion of Ru not only leads to the formation of small Ru particles, inducing some preferential exposed planes, and then favoring hydrogenation properties [40], but also to the better transportation of the reactant/product from the acid sites to the metal sites, and vice versa [16]. That probably explains the higher cracking activity of Ru supported catalysts as compared to MCM-41. Additionally, the gas yield was found to gradually increase with increasing Ru content. 2%Ru/MCM-41 produced the highest yield of gas in line with a lowest liquid yield. This might be attributed to a good balance between metal and acid sites, as a result of the high concentration of ruthenium at approximately the same dispersion, which was reported to be a crucial factor controlling the activity of a bifunctional catalyst [41]. Also, the high activity of Ru-supported catalysts leads to a drastic reduction in asphaltenes (Table 7.1).

7.4.3.2 Pyrolytic Oil

The effect of Ru loading amount can be further depicted from the petroleum cuts as shown in Figure 7.7. From the figure, the use of catalysts decreases gas oil and residues in accordance with the increment in the light fractions; naphtha and kerosene. The oils obtained over Ru-supported catalysts have higher

content of light fractions as compared to that produced over MCM-41. This is again attributed to their bifunctionality. Moreover, the contents increase with increasing Ru loading. As compared to 1.5%Ru/MCM-41, 2%Ru/MCM-41 produces the oil having slightly higher naphtha and less kerosene whereas the heavier gas oil fractions remain constant, indicating that 2%Ru/MCM-41 further cracks or transforms kerosene to naphtha and light gases.

Figure 7.8 illustrates the FTIR spectra of the derived oils. In the figure, bands at the wave number of 740cm^{-1} and 700cm^{-1} indicate the presence of the poly-aromatics including biphenyl [32,42]. As such, Ru-supported catalysts produce the oils having the lowest band intensity, indicating their low poly-aromatic contents. And the polycyclic aromatics decreases with increasing ruthenium loading. This is well consistent with the results obtained from liquid adsorption chromatography, as depicted in Figure 7.9. Besides, from the figure, a gradual increase in mono-aromatics in accordance with a decrease in poly- and polar-aromatics is observed as the ruthenium content increases. Ruthenium based catalyst was found to exhibit high hydrogenation activity [15], and its activity increased with increasing ruthenium loading [30,43]. Akhemedov and Al-Khowaiter [44] found that Ru/ZSM-5 demonstrated much higher C-C bond cleavage selectivity in cycloalkanes in comparison with alkanes. Meanwhile, the hydrogenation of aromatics occurs mostly over the metallic function of the catalyst, although the acid sites have some hydrogenation activity [45], but the rate is considerably lower than that of metal sites [46]. It was also reported that hydrogenation of polycyclic aromatics is more preferable than single-ring aromatics [46-48] and generally yields partial hydrogenated products [49]. In the present study, Ru is well dispersed in all samples, as indicated by XRD, H_2-chemisorption analysis. Therefore, it is likely that increasing Ru loading benefits a higher hydrogenation activity, promoting conversion of poly-aromatics to (partial) hydrogenated compounds, which would further undergo ring-opening and/or cracking over acid sites. As a consequence, higher concentration of mono-aromatics and light fractions are achieved.

On the other hand, the increasing ruthenium loading also leads to the gradual reduction in polar-aromatics (Figure 7.9). Several explanations might be extended to explain the polar-aromatic reduction having occurred in the cases of

Ru-supported catalysts. The increasing ruthenium content would prevent polar-aromatic formation due to the enhanced hydrogenation activity [50]. At the same time, side cracking reaction that produces polar-aromatics with lower molecular weights [51,52] might also be a candidate. And, the high amount of coke generated on the spent Ru-supported catalysts (Table 7.1) as a result of the accumulation of polar-aromatic compounds [51] should not be excluded. Besides, the increase in hydrogenation activity with increasing ruthenium content in the catalyst might promote the hydrodesulfurization (HDS) reactions, causing the reduction of polar-aromatics. This is more likely to occur since the HDS of the feed containing both polar-aromatics and other polycyclic aromatics mainly followed the HYD pathway due to the competition adsorption on the active sites [53]. And, it is also well-known that the HDS reactions via HYD pathway lead to the formation of mono-aromatic [54]. That probably explains the gradual increase in mono-aromatics at the expense of polar-aromatics as observed in Figure 7.9.

Finally, the reason for a high concentration of di-aromatics in the oil obtained over 2%Ru/MCM-41 (Figure 7.9) is not clear. However, from the FTIR analysis (Figure 7.8, the bands at the wave number of around 700cm^{-1}), it seems that the high di-aromatics content might be attributed, or at least partially, to the high concentration of bi-phenyl and its substituted compounds [45]. Therefore, it is possible that the presence of high amount of Ru sites on the very large surface of MCM-41, to a certain extent, decreases the steric hindrance, resulting in a promotion effect on the occurrence of the HDS reaction via DDS route, which is well known to produce di-aromatics [54]. Pawelec *et al.* [55] found that the HDS of 4,6 dimethyl-dibenzothiophene on CoMo/P/Ti-HMS (Hexagonal Mesoporous Silica material_HMS) catalysts occurred *via* (i) dealkylation, resulting in dibenzothiophene formation; and (ii) isomerization (main route) to produce 3,6 dimethyl-DBT, and eventually 3,4' dimethyl-biphenyl and 3,4'methylcyclohexyl toluene products. However, no study on Ru-supported pure silica MCM-41 have been published for the ability of this catalyst to drive the HDS of 4,6 dimethyl-DBT *via* the isomerization route as introduced by Pawelec [55]. But, to study this is out of the scope of this research work. Therefore, a further study is needed to elucidate this issue.

7.5 Conclusions

Catalyst temperatures strongly influenced the product distribution and the nature of the products obtained from the MCM-41 catalyzed-pyrolysis of waste tire. The oil yield first decreased, and then increased with catalyst temperature. And, under the highest studied catalyst temperature, the highest poly- and polar-aromatics were produced. In addition, increasing catalyst temperature decreased the yield of naphtha in accordance with the increment of heavier fractions. These phenomena might be attributed to the combination effects of high catalyst temperature, the meso-pore and acid properties of MCM-41, leading to the preference occurrence of alkylation, aromatization and Diel-Alder reactions.

Ru was highly dispersed in all Ru-supported catalysts. The incorporation of Ru on the surface of MCM-41 was found to have promotion effects on the catalytic activity. And the catalytic activity increased with increasing Ru loading, which was attributed to a better hydrogenation activity. Gas yield increased gradually at the expense of the liquid yields with Ru content in the bifunctional catalysts. Furthermore, Ru-supported catalysts produced much lighter oils as compared to MCM-41 and non-catalytic pyrolysis. And, a higher selectivity toward light petroleum fractions was observed over a catalyst having higher concentration of ruthenium metal sites. That was explained by the promotion in the hydrogenation of both poly- and polar-aromatics, as Ru loading increased, followed by ring-opening and/or cracking producing lower molecular weight hydrocarbons.

7.6 Acknowledgements

The Petroleum and Petrochemical Consortium (supported by MUA and ADB), Chulalongkorn University, Thailand, the Thailand Research Fund (TRF) and The Commissions on Higher Education, the Chulalongkorn University's Research Unit of "Syntheses and Applications of Organometallics" and The Graduate Scholarship Program for Faculty Members from Neighboring Countries, Chulalongkorn University are acknowledged for the partial financial support.

7.7 References

[1]. S.Galvagno, S.Casu, T. Casablanca, A. Calabrese, G. Cornacchia, Waste Manag. 229 (2002) 17-923

[2]. C. Berrueco, E. Esperanza, F.J. Mastal, J. Ceamanos, P. Garcia-Baicaicoa, J. Anal. Appl. Pyro. 74 (2005) 245-253

[3]. UK-EA, Tires in the Environment, A Technical Report by the UK Environment Agency, Bristol, UK

[4]. M.M. Barbooti, T.J. Mohamed, A.A. Hussain, F.O. Abas, J. Anal. Appl. Pyro. 72 (2004) 165-170

[5]. E. Aylon, R. Murillo, A. Fernandez-Colino, A. Aranda, T. Garcia, M.S. Callen, A.M. Mashal, J. Anal. Appl. Pyro. 79 (2007) 210-214

[6]. Paul T. Williams and David T. Taylor, Fuel 72 (1993) 1469-147

[7]. B. Benallal, C. Roy, H. Pakdel, S. Chabot, M.A. Poirier, Fuel. 74 (1995) 1589-1594

[8]. A.M. Cunliffe, P.T. Williams, J. Anal. Appl. Pyro. 44 (1998) 131-152

[9]. P.T. Williams, R.P. Bottrill, Fuel 74 (1995) 736-742

[10]. P.T. Williams, A.J. Brindle, Fuel 81(2002) 2425-2434

[11]. P.T. Williams and A.J. Brindle, J. Anal. Appl. Pyro. 67 (2003) 143-164

[12]. S. Boxiong, W. Chunfei, G. Binbin, W. Rui, Liangcai, Appl. Catal. B: Environ. 73 (2007) 150-157

[13]. N.A. Dũng, A. Mhodmonthin, S. Wongkasemjit, and S. Jitkarnka, J. Anal. Appl. Pyro. 85 (2009) 338-344

[14]. A. Lugstein, A. Jentys, H. Vinek, Appl. Catal. A: Gen. 176 (1999) 119-128

[15]. M.A. Ali, T. Kimura, Y. Suzuki, M.A. Al-Saleh, H. Hamid, T. Inui, Appl. Catal. A: Gen. 277 (2002) 63-72.

[16]. D. Eliche-Quesada, J.M. Meria-Robles, E. Rodriguez-Castellon, A. Jimenez-Lopez, Appl. Catal. B: Environ. 65 (2006) 118-126

[17]. D. Eliche-Quesada, M.I. Macias-Ortiz, J.Jimenez-Jimenez, E. Rodriguez-Castellon, A. Jimenez-Lopez, J. Mole. Catal. A: Chemical 225 (2006) 41-48

[18]. J.B. McKinley, In: Emett PH, editor. Catalysis, vol. 5. Nework: Reinhold, 1957

[19]. T.A. Pecoraro and R.R. Chianelli, J. Catal. 67 (1981) 430-445

[20]. J. Barbier, E. Lamy-Pitara, P. Maracot, J.P. Boitiaux, J. Cosyns, F. Verna, Adv. Catal. 37 (1990) 279-318

[21]. J.K. Lee, H.K. Rhee, J. Catal. 177 (1998) 208-216

[22]. E. Rodriguez-Castellon, J. Merida-Robles, L. Diaz, p. Maireles-Torres, J.J. Jones, J. Roziere, A. Jemenez-Lopez, Appl. Catal. A: Gen. 260 (2004) 9-18

[23]. Y. Sakata, M.A. Uddin, A. Muto, Y. Kanada, K. Koizumi, K. Murata, J. Anal. Appl. Pyro. 43 (1997) 15-25

[24]. M.A. Uddin, Y. Sakata, A. Muto, Y. Shiraga, K. Koizumi, Y. Kanada, K. Murata, Micro. Meso. Materials. 21 (1998) 557-564

[25]. Z.S. Seddegi, U. Budrthumal, A.A. Al-Arfaj, A.M. Al-Amer, S.A.I. Barri, Appl. Catal. A: Gen. 225 (2002) 167-176

[26]. Boxiong Shen, Chunfei Wu, Rui Wang, Binbin Guo, Cai Liang, J. Hazard. Mater. 137 (2006) 1065-1073

[27]. W. Charoenpinijkarn, M. Sawankruhasn, B. Kesapabutr, S. Wongkasemjit, A.M. Jamieson, J. Polym. 37 (2001) 1441–1448

[28]. N. Thanabodeekij, S. Sadthayanon, E. Gulari, S. Wongkasemjit, Materials Chemistry and Physics. 98 (2006) 131-137

[29]. G. Sebor, J. Blaz ek, M.F. Nemer, J. Chromatogr A, 847 (1999) 323-330

[30]. Eliche-Quesada, J.M Merida-Robles, E. Rodríguez-Castellon, A. Jiménez-Lopez, Appl. Catal. A: Gen. 279 (2005) 209-221

[31]. S.H. Wang and P.R. Griffiths, Fuel 64 (1985) 229-265

[32]. C.A. Islas-Flores, E. Buenrostro-Gonzalez, C. Lira-Galeana, Fuel 85 (2006) 1845-1850

[33]. L. Zhichang, M. Xianghai, X. Chunming, G. Jensen, Chin. J. Chem. Eng. 15 (2007) 309-314.

[34]. X. Meng, C. Xu, J. Gao, Lili, Appl. Catal. A: Gen. 294 (2005) 168-176

[35]. J.J McKetta, Chemical Processing Handbook, Marcel Dekker Inc, NewYork, 1993

[36]. Z. Zhao, W. Qiao, X. Wang, G. Wang, Z. Li, L. Cheng, Micro. Meso. Mat. 94 (2006) 105-112

[37]. G. San Miguel, J. Aguado, D.P. Serrano, J.M. Escola, Appl. Catal. B:

Environ. 64 (2006) 209-219

[38]. K.H. Lee, Y.W. Lee, and B.H. Ha, J. Catal. 178 (1998) 328-337

[39]. P.B. Venuto and T.E. Habib, Fluid catalytic cracking with zeolite catalysts, Marcel Dekker, New York 1979

[40]. R.M. Navarro, P. Castano, M.C. Alvarez-Galvan, B. Pawelec, Catal. Today. 143 (2009) 108 – 114.

[41]. A. Soualah, J.L. Lemberton, L. Pinard, M. Chater, P. magnoux, K. Moljord, Appl. Catal. A: Gen. 336 (2008) 23-28

[42]. C. Jager, F. Huisken, H. Mutschke, Th. Henning, W. Poppitz, I. Voicu, Carbon 45 (2007) 2981-2994

[43]. D. Eliche-Quesada, E. Rodriguez-Castellon, A. Jimenez-Lopez, Micro. Meso. Mat. 99 (2007) 268-278

[44]. V.M. Akhmedov, S.H. Al-Khowaiter, Appl. Catal. A: Gen. 197 (2000) 201-212

[45]. O. Cairon, K. Thomas, A. Chambellan, T. Chevreau, Appl. Catal. A: Gen. 238 (2003) 167-183

[46]. P. Castano, B. Pawelec, J.L.G. Fieero, J.M. Arandes, J. Bilbao, Appl. Catal. A: Gen. 315 (2006) 101-113

[47]. A. Corma, A. Martinez, and V. Martinez-Soria, J. Catal. 169 (1997) 480-489

[48]. S. Jongpatiwut, Z. Li, D. E. Resasco, W.E. Alvarez, Ad L. Sughrue, G.W. Dodwell, Appl. Catal. A: Gen. 262 (2004) 241-253

[49]. M. Jacquin, D.J. Jones, J.Roziere, S.Albertazzi, A.Vaccari, M. Lenarda, L. Storaro, R. Ganzerla, Appl. Catal. A: Gen. 251 (2003) 131-141

[50]. Nguyễn Anh Dũng, Sujitra Wongkasemjit, Sirirat Jitkarnka, Effects of pyrolysis temperature and Pt-loaded catalysts on polar-aromatic content in the tire-derived oil, Appl. Catal. B: Environ. In Press DOI:10.1016/j.apcatb.2009.05.038

[51]. A. Corma, C. Martinez, G. Ketley and G. Blair, Appl. Catal. A: Gen. 208 (2001) 135-152

[52]. J.A. Valla, A.A. Lappas and I.A. Vasalos, Appl. Catal. A: Gen. 297 (2006) 90-101

[53]. H.Pakdel. D.M. Pantea and C. Roy, J. Anal. Appl. Pyro. 57 (2001) 91-107

[54]. H. Wang and R. Prins, J. Catal. 258 (2008) 153-164

[55]. B. Pawelec, J.L.G. Fierro, A. Montesinos, T.A. Zepeda, Appl. Catal. B: Environ. 80 (2008) 1-14.

Table 7.1 Physical and chemical properties of MCM-41 and Ru-supported catalysts

Samples	%wt Ru	Dispersion (%)	Ru particle size[b] (nm)	Surface area ($m^2 g^{-1}$)	Pore Diameter (nm)	Coke ($g g^{-1}$ catalyst)	Asphaltenes ($g g^{-1}$ oil)
MCM-41 (350°C)[a]	-	-	-	1454	2.61	0.084	0.00064
MCM-41 (400°C)[a]	-	-	-	1454	2.61	0.097	0.00053
MCM-41 (450°C)[a]	-	-	-	1454	2.61	0.108	0.00073
1%Ru/MCM-41	0.98	68.5	1.88	1450	2.57	0.119	0.00048
1.5%Ru/MCM-41	1.51	67.9	1.90	1448	2.56	0.126	0.00041
2%Ru/MCM-41	2.02	65.2	1.98	1439	2.51	0.124	0.00022

[a]Catalyst temperature

[b] Mean diameter of ruthenium particle determined by H_2-chemisorption

Table 7.2 Products obtained from thermal and catalytic pyrolysis using MCM-41*

Yield (%wt)	Non-Cat	MCM-41	Content (%wt)	Non-Cat	MCM-41	Yield (%wt)	Non-Cat	MCM-41
Naphtha	13.02	18.81	Sat-HCs	53.81	48.21	Gas	10.33	14.56
Kerosene	8.81	9.95	Mono-aromatics	13.24	17.18	Liquid	44.02	38.02
LGO	7.80	4.83	Di-aromatics	9.88	20.37	Solid	45.65	45.42
GO	7.62	2.28	Poly-aromatics	8.99	6.55			
Residues	6.77	2.15	Polar-aromatics	12.68	7.69			

*Catalyst temperature = 350°C

Table 7.3 Pyrolysis products obtained from using various catalytic temperatures

Catalyst Temperature (°C)	Product Distribution (%wt)			Yield of Petroleum Cuts (%wt)				Chemical Composition (%wt)	
	Gas	Liquid	Solid	Naphtha	Kerosene	Gas Oil	Residues	Poly-aromatics	Polar-aromatics
(Non-Cat) 350	10.33	44.02	45.65	13.02	8.81	15.42	6.77	8.99	12.68
350	14.56	38.02	45.42	18.81	9.95	7.11	2.15	6.55	7.69
400	23.52	32.05	45.24	16.49	8.38	5.88	1.11	6.45	8.05
450	13.52	42.04	44.44	15.64	10.61	13.08	2.35	8.21	11.69

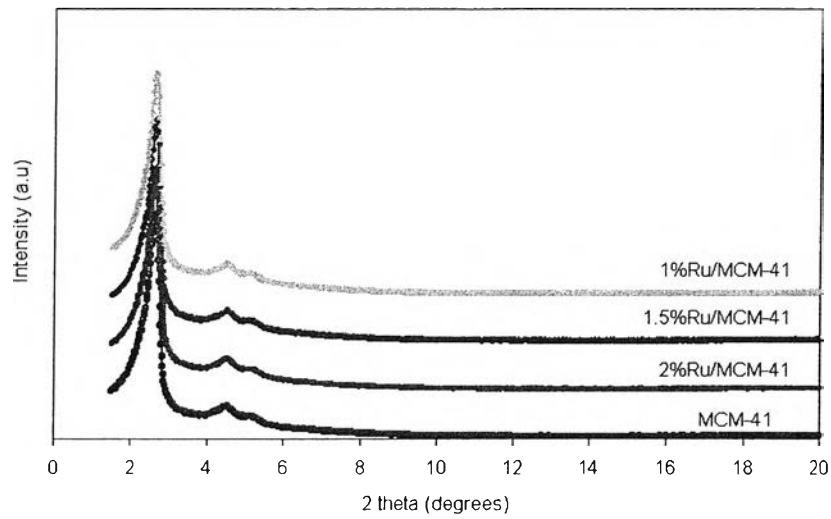

Figure 7.1 XRD patterns of the MCM-41 and Ru/MCM-41 catalysts.

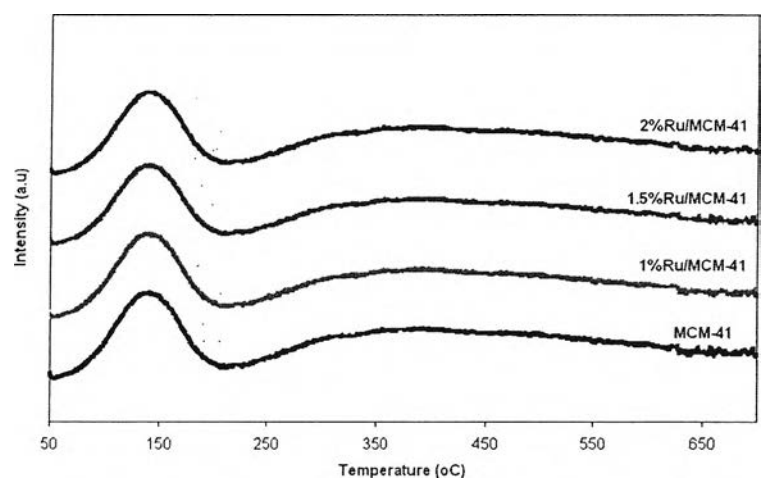

Figure 7.2 TPD-NH_3 profiles of Ru/MCM-41 catalysts.

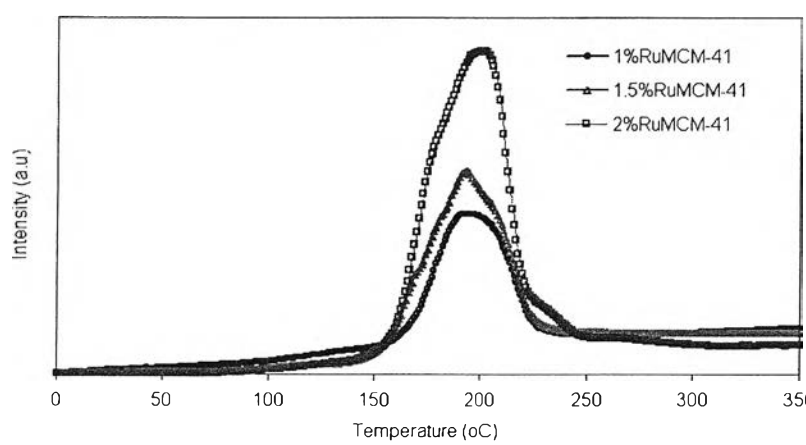

Figure 7.3 TPR profiles of Ru/MCM-41 catalysts at various loading percentages.

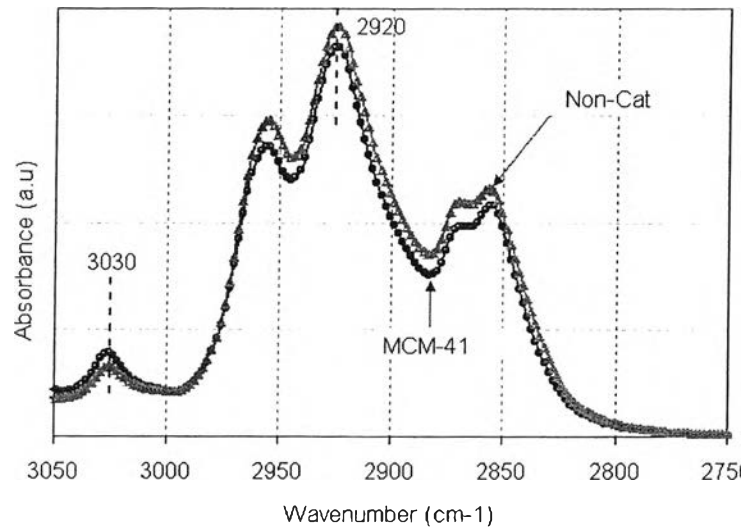

Figure 7.4 IR spectra of pyrolytic oils obtained from thermal and catalytic pyrolysis using MCM-41 at 350°C.

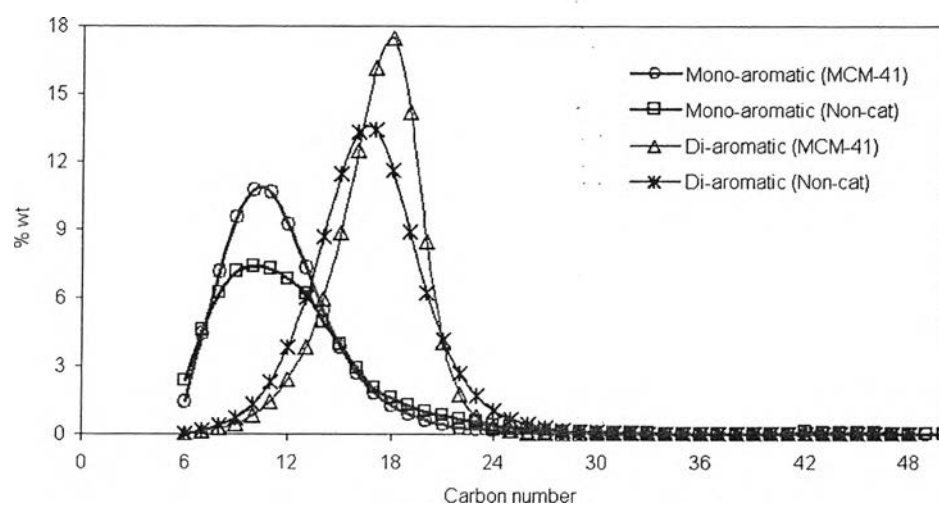

Figure 7.5 Carbon number distribution of mono- and di-aromatics in oils obtained from thermal and catalytic pyrolysis using MCM-41.

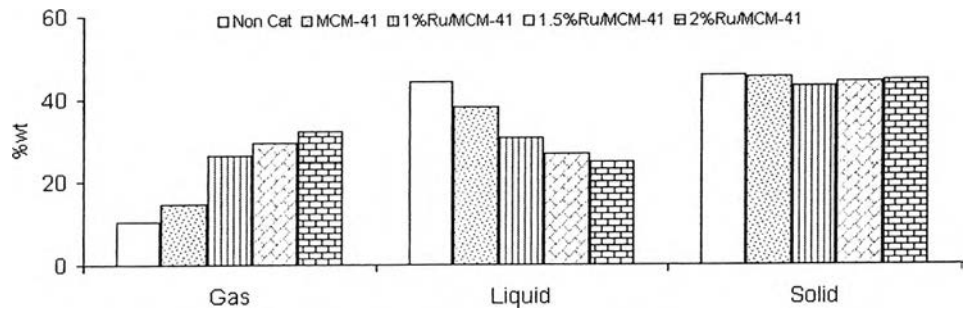

Figure 7.6 Effect of Ru loading amount on product distribution.

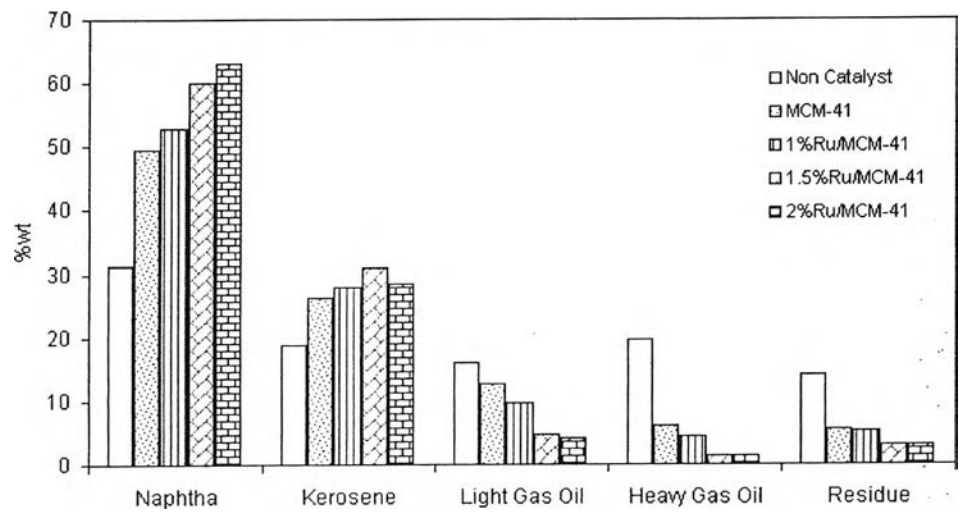

Figure 7.7 Petroleum cuts of pyrolytic oils obtained from using various Ru percentages.

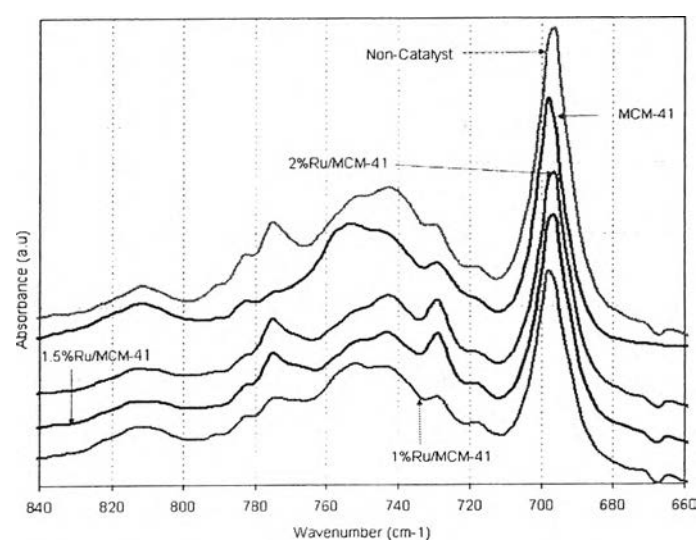

Figure 7.8 IR spectra of pyrolytic oils obtained from thermal and catalytic pyrolysis.

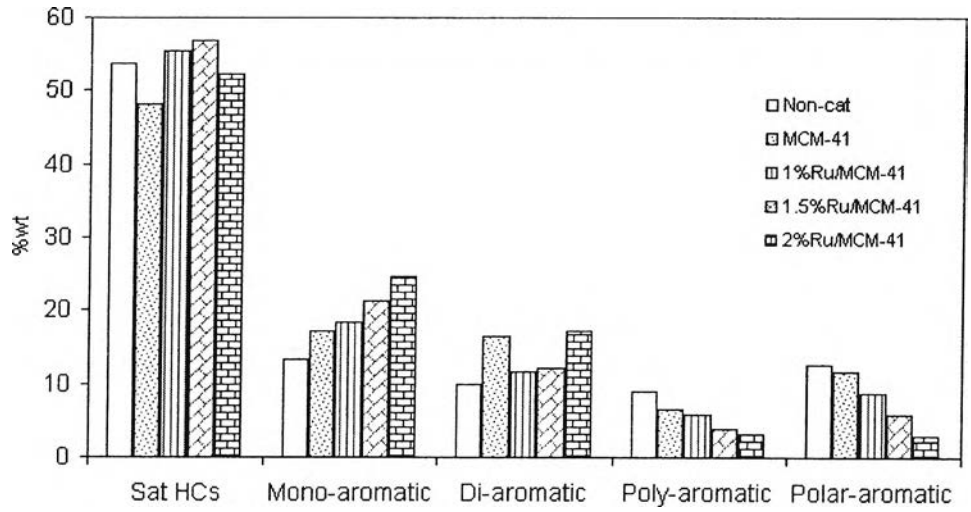

Figure 7.9 The chemical compositions of pyrolytic oils obtained from thermal and catalytic pyrolysis.